XVIII International Conference on Water Resources
CMWR 2010
J. Carrera (Ed)

NUMERICAL UPSCALED MODEL OF TRANSPORT WITH NON-SEPARATED SCALE

Son-Young Yi*, Małgorzata Peszyńska† and Ralph E. Showalter†

*The University of Texas at El Paso(UTEP)
El Paso, TX 79968, USA
e-mail: syi@utep.edu

† Oregon State University
Corvallis, OR 97331, USA
e-mail: {mpesz,show}@math.oregonstate.edu

Key words: Upscaled model, Double-porosity, Solute transport, Non-separated scale, Memory terms.

Summary. We study numerically a new model describing the multiscale flow of a single-phase incompressible fluid and transport of a dissolved chemical by advection and diffusion through a heterogeneous porous medium without the usual assumptions of scale separation. The new model includes as special cases the classical homogenized model as well as the double porosity models, but is characterized by presence of additional memory terms which describe the effects of local advective transport as well as diffusion. We discuss numerical discretizations and present numerical results to show the quantitative significance of each memory term in different regimes of flow and transport.

1 INTRODUCTION

Let Ω be a two-dimensional heterogeneous porous medium containing two disjoint flow regims. The subscripts f and s are associated with the fast and slow regions Ω_f and Ω_s, respectively. The region Ω_f is connected, but $\Omega_s = \cup_{i=1}^{\mathbb{N}_{incl}} \Omega_{is}$ is a union of disjoint connected regions Ω_{is}.

Assume that Ω is covered by a union of rectangular subdomains Ω_i, $i = 1, \ldots, \mathbb{N}_{incl}$, with each Ω_{is} containing exactly one inclusion Ω_{is}. Let $\Omega_{if} = \Omega_i \cap \Omega_f$ be the fast part surrounding Ω_{is} and let $\Gamma_i = \partial\Omega_{is} \cap \partial\Omega_f$ denote the local interfaces so that $\Omega_i = \Omega_{is} \cup \Omega_{if} \cup \Gamma_i$. Let us assume that each Ω_i is congruent to a generic cell Ω_0 which contains the fast flow region Ω_{0f} surrounding the slow flow region Ω_{0s}. We also denote the volume fraction of the fast part by $\theta_f = \frac{|\Omega_{0f}|}{|\Omega_0|}$ and analogously $\theta_s = \frac{|\Omega_{0f}|}{|\Omega_0|} = 1 - \theta_f$.

Now we describe the microscopic model of the flow and solute transport in the heterogeneous porous media, with porosity and permeability discontinuous across the interface

Γ_{fs}. The flow in porous media is described by conservation of mass and Darcy's law:

$$\nabla \cdot \mathbf{v}_f = 0, \qquad \mathbf{v}_f = -\mathbf{K}_f \nabla p_f, \qquad \mathbf{x} \in \Omega_f, \tag{1a}$$

$$\nabla \cdot \mathbf{v}_i = 0, \qquad \mathbf{v}_i = -\mathbf{K}_s \nabla p_i, \qquad \mathbf{x} \in \Omega_{is},\ i = 1, \ldots, \mathbb{N}_{incl}, \tag{1b}$$

$$p_i = p_f, \qquad \mathbf{v}_i \cdot \mathbf{n} = \mathbf{v}_f \cdot \mathbf{n}, \qquad \mathbf{x} \in \Gamma_i, \tag{1c}$$

where $\mathbf{v}$ and p is the velocity and the pressure of the flow, respectively. The coefficient K is the permeability of the porous medium. The solute transport equation is an advection-diffusion-dispersion equation as follows:

$$\phi_f \frac{\partial c_f}{\partial t} - \nabla \cdot (\mathbf{D}_f \nabla c_f - \mathbf{v}_f c_f) = 0, \quad \mathbf{x} \in \Omega_f, \tag{2a}$$

$$\phi_i \frac{\partial c_i}{\partial t} - \nabla \cdot (\mathbf{D}_i \nabla c_i - \mathbf{v}_i c_i) = 0, \quad \mathbf{x} \in \Omega_{is},\ i = 1, \ldots, \mathbb{N}_{incl}, \tag{2b}$$

$$c_i = c_f, \quad (\mathbf{D}_f \nabla c_f - \mathbf{v}_f c_f) \cdot \mathbf{n} = (\mathbf{D}_i \nabla c_i - \mathbf{v}_i c_i) \cdot \mathbf{n}, \qquad \mathbf{x} \in \Gamma_i. \tag{2c}$$

Here, c is the solute concentration and ϕ is the porosity of the medium. The diffusion-dispersion tensor is given by

$$\mathbf{D} = \mathbf{D}(\mathbf{v}) \equiv d_{\text{mol}}\mathbf{I} + |\mathbf{v}|(d_l \mathbf{E}(\mathbf{v}) + d_t(\mathbf{I} - \mathbf{E}(\mathbf{v}))). \tag{3}$$

Here d_{mol}, d_l, d_t are coefficients of molecular diffusivity, longitudinal and transversal dispersivity, respectively, and the dispersion tensor $\mathbf{E}(\mathbf{v}) = \frac{1}{|\mathbf{v}|^2} v_i v_j$ is a rank two tensor.

2 THE UPSCALED COUPLED FLOW-ADVECTION-DIFFUSION MODEL WITH MEMORY TERMS

We shall describe the discrete version of the double-porosity model with various memory terms for the coupled flow-transport equation as developed in [1]. To describe the upscaled flow equation, we first define the upscaled permeability tensor $\mathbf{K}^*$ as follows:

$$(\mathbf{K}^*)_{jk} = \frac{1}{|\Omega_0|} \int_{\Omega_{0f}} K_{jm}(\mathbf{y})(\delta_{mk} + \partial_m \omega_k(\mathbf{y}))\, dA, \tag{4}$$

where Ω_0-periodic function $\omega_k(\mathbf{y})$ is defined as the solution of the cell problem

$$\begin{cases} -\nabla \cdot \nabla \omega_j(\mathbf{y}) = 0, & \mathbf{y} \in \Omega_{0f} \\ \nabla \omega_j(\mathbf{y}) \cdot \mathbf{n} = -\mathbf{e}_j \cdot \mathbf{n}, & \mathbf{y} \in \Gamma_{fs}. \end{cases} \tag{5}$$

The discrete double-porosity model that we employ here uses the local affine approximation on the interfaces which enables the model to capture the effects of advection and secondary diffusion. The upscaled flow model can be described by the following system of equations using a coefficient $\overline{\mathbf{K}^*} = \mathbf{K}^* + \theta_s \mathbf{K}_s$

$$\nabla \cdot \overline{\mathbf{v}^*} = 0, \qquad \overline{\mathbf{v}^*} = -\overline{\mathbf{K}^*}\nabla p^*, \qquad \mathbf{x} \in \Omega, \tag{6a}$$

$$\nabla \cdot \mathbf{v}_i^* = 0, \qquad \mathbf{v}_i^* = -\mathbf{K}_s \nabla p_i^*, \qquad \mathbf{y} \in \Omega_i,\ i = 1, \cdots, \mathbb{N}_{incl}, \tag{6b}$$

$$p_i^*|_{\Gamma_i} = (\Pi_1(p^*))_i, \tag{6c}$$

where the operator Π_1 is the local affine approximation.

To describe the upscaled transport system with memory terms in a convolution form, we define auxiliary functions as follows, for every $i = 1, \cdots, \mathbb{N}_{incl}$,

$$\phi_i \frac{\partial r_i^0}{\partial t} - \nabla \cdot (\mathbf{D}_i \nabla r_i^0 - \mathbf{v}_i^* r_i^0) = 0, \qquad \mathbf{y} \in \Omega_{is} \tag{7a}$$

$$r_i^0(\mathbf{y}, 0) = 0, \qquad \mathbf{y} \in \Omega_{is} \tag{7b}$$

$$r_i^0(\mathbf{y}, 0) = 1, \qquad \mathbf{y} \in \Gamma_i. \tag{7c}$$

For $k = 1, 2$,

$$\phi_i \frac{\partial r_i^k}{\partial t} - \nabla \cdot (\mathbf{D}_i \nabla r_i^k - \mathbf{v}_i^* r_i^k) = 0, \qquad \mathbf{y} \in \Omega_{is} \tag{8a}$$

$$r_i^k(\mathbf{y}, 0) = 0, \qquad \mathbf{y} \in \Omega_{is} \tag{8b}$$

$$r_i^k(\mathbf{y}, 0) = (\mathbf{y} - \mathbf{x}_{0i}^c)_k, \qquad \mathbf{y} \in \Gamma_i. \tag{8c}$$

Here $\mathbf{x}_{0i}^c$ the center of Ω_{is}.

We use kernels arising from various averages of r^k. First, we use the averages of rate of change in time

$$\mathcal{T}_i^{k0}(t) \equiv \frac{1}{|\Omega_i|} \int_{\Omega_{is}} \phi_s \frac{\partial r_i^k}{\partial t}(\mathbf{y}, t)\, dA, \quad k = 0, 1, 2 \tag{9}$$

Next, the kernels $\mathcal{T}_i^{k1}, \mathcal{T}_i^{k2}$ arising from the first moments of $r_i^k, k = 0, 1, 2$, are defined by

$$\mathcal{T}_i^{kj}(t) \equiv \frac{1}{|\Omega_i|} \int_{\Omega_{is}} \phi_s \frac{\partial r_i^k}{\partial t}(\mathbf{y}, t)(\mathbf{y} - (\mathbf{x}_{0i}^C))_j\, dA, \quad j = 1, 2;\ k = 0, 1, 2. \tag{10}$$

Finally, for each $r_i^k, k = 0, 1, 2$ we set

$$\mathbf{S}_i^k(t) \equiv \frac{1}{|\Omega_i|} \int_{\Omega_{is}} \left(\mathbf{D}_i \nabla r_i^k(\mathbf{y}, t) - \mathbf{v}_i^* r_i^k(\mathbf{y}, t) \right) dA. \tag{11}$$

Let $\mathbb{N}_{incl}$ be large and let us suppress the dependence of the kernels on i. Then the limiting model of the transport systems with memory terms in convolution form is

$$\begin{aligned}\phi^*\frac{\partial c^*}{\partial t} + \mathcal{T}^{00} * \frac{\partial c^*}{\partial t} \\ + (\mathcal{T}^{10}, \mathcal{T}^{20}) * \nabla\frac{\partial c^*}{\partial t} - \nabla\cdot\left((\mathcal{T}^{01}, \mathcal{T}^{02}) * \frac{\partial c^*}{\partial t}\right) - \nabla\cdot\left((S^{01}, S^{02}) * \frac{\partial c^*}{\partial t}\right) \\ - \nabla\cdot\left(\begin{bmatrix} \mathcal{T}^{11} & \mathcal{T}^{12} \\ \mathcal{T}^{21} & \mathcal{T}^{22} \end{bmatrix} * \nabla\frac{\partial c^*}{\partial t}\right) - \nabla\cdot\left(\begin{bmatrix} S^{11} & S^{12} \\ S^{21} & S^{22} \end{bmatrix} * \nabla\frac{\partial c^*}{\partial t}\right) \\ - \nabla\cdot(\mathbf{D}^*\nabla c^* - \mathbf{v}^* c^*) = 0, \quad (12)\end{aligned}$$

where the effective porosity $\phi^* = \theta_f\phi_f$. After we collect like-terms, the above equation (12) can be written in a compact form:

$$\phi^*\frac{\partial c^*}{\partial t} + \mathcal{T}^{00} * \frac{\partial c^*}{\partial t} + \mathbf{M} * \nabla\frac{\partial c^*}{\partial t} - \nabla\cdot\left(\mathcal{M} * \nabla\frac{\partial c^*}{\partial t}\right) - \nabla\cdot(\mathbf{D}^*\nabla c^* - \mathbf{v}^* c^*) = 0, \quad (13)$$

where $\mathbf{M} : (0,\infty) \to \mathbb{R}^2, \mathcal{M} : (0,\infty) \to \mathbb{R}^{2\times 2}$ are time dependent vector and matrix valued memory kernels.

3 NUMERICAL DISCRETIZATION

In this section, we describe a numerical method called Locally Conservative Eulerian-Lagrangian Method (LCELM) that was used to discretize the systems (7) and (8) and the effective solute transport equation (13). LCELM is a numerical technique that has been developed for convection-dominated diffusive systems and is based on the operator splitting technique. Originally, LCELM was introduced to achieve the local conservation of mass for the problem of two-phase, immiscible, incompressible flow in porous media [2] and its convergence of a version of LCELM as applied to a semilinear parabolic problem in one and two space variables has been proved [3, 4].

3.1 Locally Conservative Eulerian-Lagrangian Method

Consider the following initial value problem for an advection-diffusion equation:

$$\nabla_{t,\mathbf{x}}\cdot\begin{pmatrix}\phi s(\mathbf{x},t)\\ \mathbf{u}(\mathbf{x},t)\end{pmatrix} - \nabla\cdot(\mathbf{D}\nabla s) + g(s) = 0,\ \mathbf{x}\in\Omega,\ 0\le t\le T. \quad (14)$$

We want to compute an approximate solution S to s at each discrete time step. Let $\{M_{ij}\}$ be the rectangular partition of uniform size $h_x \times h_y$ of Ω. In order to define a predecessor set for M_{ij}, let $\mathbf{y}(t;\mathbf{x})$ be the solution of the final value problem given by

$$\mathbf{y}' = \mathbf{u}/\phi \text{ and } \mathbf{y}(t^n,\mathbf{x}) = \mathbf{x}. \quad (15)$$

Then, let

$$\partial\tilde{M}_{ij}^n = \{\mathbf{y}(t^{n-1};\mathbf{x}) : \mathbf{x} \in \partial M_{ij}\}, \tag{16}$$

and define the interior of $\partial\tilde{M}_{ij}^n$ to be the predecessor set $\tilde{M}_{ij}$ at time t^{n-1} corresponding to M_{ij} at time t^n. Define the tube E_{ij}^n to be the set interior to $M_{ij}, \tilde{M}_{ij}^n$ and the lateral boundary F_{ij}^n defined by the integral curve $\mathbf{y}(t;\mathbf{x}), t^{n-1} < t < t^n$, $\mathbf{x} \in \partial M_{ij}$. Then, the solution of (14) satisfies the relation

$$\int_{M_{ij}} \phi S^n \, d\mathbf{x} - \int_{\tilde{M}_{ij}} \phi S^{n-1} \, d\mathbf{x} - \int_{D_{ij}^n} \nabla \cdot (\mathbf{D}\nabla s) \, d\mathbf{x}dt + \int_{D_{ij}^n} g(s) \, d\mathbf{x}dt = 0. \tag{17}$$

In order to approximate the transport part, the sets $\tilde{M}_{ij}^n$ and E_{ij}^n must be approximated. Define an approximate predecessor $\widehat{Q}_{ij}^n$ as the quadrilateral having vertices $\widehat{\mathbf{x}}_{ij,k}^n = \mathbf{x}_{ij,k} - \frac{\mathbf{u}(\mathbf{x}_{ij,k},t^n)}{\phi}\Delta t$, where $\mathbf{x}_{ij,k}$, $k = 1, \cdots 4$, are the vertices of M_{ij}.

Let $\widehat{E}_{ij}^n$ be the tube formed with top M_{ij} and bottom $\widehat{Q}_{ij}^n$. Then, the approximate solution $\overline{S}$ to the transport part of (14) can be computed as follows:

$$\int_{M_{ij}} \overline{S}_{ij}^n \, d\mathbf{x} = \int_{\widehat{Q}_{ij}^n} S^{n-1} \, d\mathbf{x}. \tag{18}$$

Next, we approximate the solution of the diffusive part by a cell-centered finite difference method as follows.

$$\begin{aligned} &h_x^2 h_y^2 \phi(S_{ij}^n - \overline{S}_{ij}^n) - (\Delta t) h_y^2 \mathbf{D}_{11}(S_{(i+1)j}^n + S_{(i-1)j}^n - 2S_{ij}^n) \\ &\quad - (\Delta t) h_x^2 \mathbf{D}_{22}(S_{i(j+1)}^n + S_{i(j-1)}^n - 2S_{ij}^n) + (\Delta t) h_x^2 h_y^2 g(S_{ij}^n) = 0. \end{aligned} \tag{19}$$

When we apply LCELM to the upscaled transport equation (13), all the convolution terms are treated in $g(c^*)$. We will approximate the convolution terms using the method developed by Peszyńska [5].

3.2 Approximation of the convolution terms

Let us consider a convolution term of the following form:

$$u_t * \tau(t) = \int_0^t u_t(\mathbf{x}, s)\tau(t-s) \, ds, \mathbf{x} \in \Omega, t \in I = (0, T). \tag{20}$$

The convolution kernel $\tau(\cdot)$ is related to the microscopic properties of the domain of the flow. Define the partition of I as follows; Let $N \geq 0$ be integer, $\Delta t = \frac{T}{N}$ be the time step, let $t^k = k\Delta t$, $k = 0, \cdots, N$, and $I = \cup_{k=1}^N I^k$, $\quad I^k = (I^{k-1}, I^k]$. We denote the characteristic function of the subinterval I_k by θ^k and define a family of functions: $\{\xi^k\}_{k=1}^N$ as follows:

$$\xi^k(t) = \int_0^t \tau(t-s)\theta^k(s) \, ds \tag{21}$$

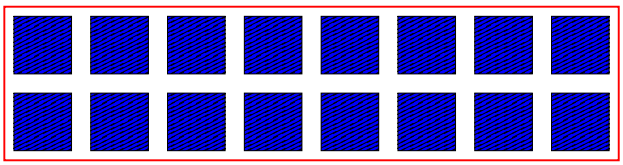

Figure 1: Computational domain Ω.

and we define also

$$\eta^{i,k} = \frac{1}{\Delta t}\int_{t^{i-1}}^{t^i} \xi^k(t)\,dt, \quad 1 \le i,k \le N. \tag{22}$$

Then we approximate $u_t * \tau(t)$ at time t^i as follows:

$$(u_t * \tau)(t^i) = \sum_{k=1}^{i} \eta^{i,k}\frac{u^k - u^{k-1}}{\Delta t}. \tag{23}$$

4 NUMERICAL RESULTS

In this section, we present our computational results for the upscaled coupled equations (6) and (13). Our domain Ω is a rectangle of size $80 \times 20\,cm^2$. Let the generic cell Ω_0 be a square of size $l \times l$, and Ω_{0s}, centered inside Ω_0, be a square of size $(l-\delta)\times(l-\delta)$. Therefore, the fast flow part Ω_{0f} has uniform thickness around Ω_{0s}. The porosity of Ω_f is $\phi_f = 0.45$ and the porosity of Ω_s is $\phi_s = 0.4$. We consider three different regimes of flow and transport depending on the ratio $\mathbf{K}_{ratio} = \mathbf{K}_f/\mathbf{K}_s$. These are $\mathbf{K}_{ratio} = 6, 300, 1800$ and are called the low, intermediate, and high contrast cases, respectively. We assume that the permeability $\mathbf{K}_f$ is isotropic and $\mathbf{K}_f = 5.78822 \cdot 10^{-2}\,cm/s$. We also assume that the medium is initially fully concentrated with the solute, i.e. $c^* = 1$, $t = 0$, $\mathbf{x} \in \partial\Omega$ and clear fluid is pumped into the medium at the left boundary, that is $c^* = 0$, $t > 0$, $\mathbf{x} \in \partial\Omega_{left}$. We impose no-flow conditions on $\mathbf{v}_f$ along the top and bottom of the porous medium and $\mathbf{v}_f \cdot \mathbf{n} = v_l = 15\,cm$ along the left boundary and $\mathbf{v}_f \cdot \mathbf{n} = v_r = 15\,cm$ along the right boundary of the medium. In this case, the flow is an 1-D flow from left to right and can be easily computed. In our simulation, we approximate the effective permeability as follows: $\mathbf{K}^* = \frac{1}{l^2}(\delta^2 + (l-\delta)\delta)\cdot\mathbf{K}_f = \frac{\delta}{l}\cdot\mathbf{K}_f$. The effective diffusion/dispersion tensor is computed in the same way, *i.e.* $\mathbf{D}^* = \frac{\delta}{l}\mathbf{D}_f$. Then we can compute $\mathbf{v}^* = (v_l\mathbf{K}^*/(\mathbf{K}^* + \theta_s\mathbf{K}_s), 0)$ and $\mathbf{v}_i^* = (v_l\mathbf{K}_s/(\mathbf{K}^* + \theta_s\mathbf{K}_s), 0)$ follows. We summarize our effective parameters for each flow regime in the Table 2.

We shall present the breakthrough curves of the solute at the right side of the medium in three different contrast cases at the final time $T = 10$. Figure 2 shows the breakthrough curves using four different models; the obstacle problem, the traditional double porosity model, the model which includes the secondary diffusion term and the full model which

Domain $[cm^2 \times h]$	$\Omega = [0, 80] \times [0, 20]$	T=[0,10]	
Generic cell $[cm]$	$l = 10$	$\delta = 2$	
Porosity [-]	$\phi_f = 0.45$	$\phi_s = 0.4$	
Permeability $[cm/h]$	$K_f = 5.78822 \cdot 10^{-2}$	$K_s = \mathbf{K}_{ratio} \cdot K_f$	
Diff/Disp $[cm^2/h]$	$D_{mol} = 0.252$	$D_{trans} = 0.0$	$D_{long} = 1.224$
Number of Elements	$N_x \times N_y = 16 \times 64$	$n_x \times n_y = 64 \times 64$	
Time step [h]	$\Delta t = 4.883 \cdot 10^{-3}$	$\delta t = 1.221 \cdot 10^{-3}$	

Table 1: Simulation parameters

Parameter	Low	Intermediate	High
$\phi^* [-]$	0.2880	0.2880	0.2880
$\mathbf{K}^* [cm/h]$	$1.1576 \cdot 10^{-2}$	$1.1576 \cdot 10^{-2}$	$1.1576 \cdot 10^{-2}$
$\mathbf{v}^* [cm/h]$	11.5384	14.9105	14.9850
$\mathbf{v}_i^* [cm/h]$	9.6157	0.2485	0.0416

Table 2: Effective parameters in three different flow regimes

includes all memory terms. We observe different tailing effects due to different memory terms. In high and intermediate contrast cases, the secondary diffusion and the secondary advection terms do not seem to play an important role and, therefore, the traditional double-porosity model yields fairly good results. However, in the low contrast case, each memory term gives rise to a noticeable difference in the breakthrough curve. Moreover, breakthrough curves from different permeability heterogeneity display different tailing behaviors which are even clearer on a log-log scale in Figure 3. No significant tailing occurs in the low contrast case. In the high contrast case the tailing is long-term and diffusion driven, while the intermediate contrast case shows flatter early part of tails which are primarily advective. These phenomena coincide with the observation made in lab experiments [6]. We will discuss some properties of the memory kernels and the analysis of the numerical methods used in this work in a forthcoming paper.

REFERENCES

[1] Małgorzata Peszyńska and Ralph E. Showalter, Multiscale elliptic-parabolic systems for flow and transport, *Electron. J. Differential Equations*, **247**(30): (electronic) (2007).

[2] J. Douglas, Jr., F. Pereira, and L. M. Yeh, A locally conservative Eulerian-Lagrangian numerical method and its application to nonlinear transport in porous media, *Computational Geosciences*, **4**, 1–40 (2000).

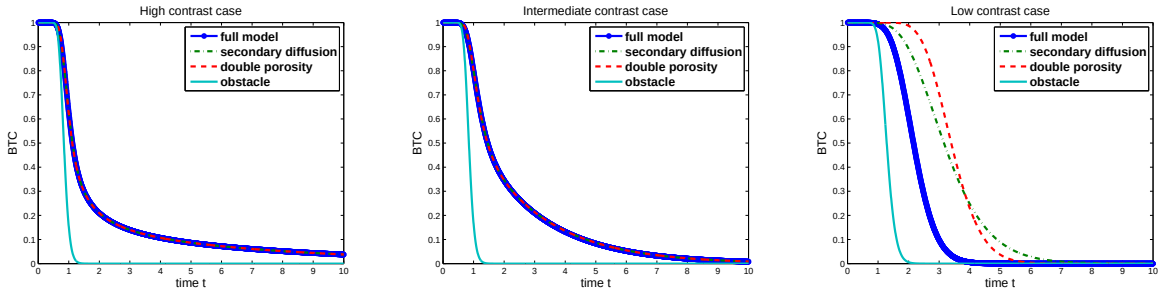

Figure 2: Breakthrough curves using various models in high, intermediate, and low contrast cases from left to right.

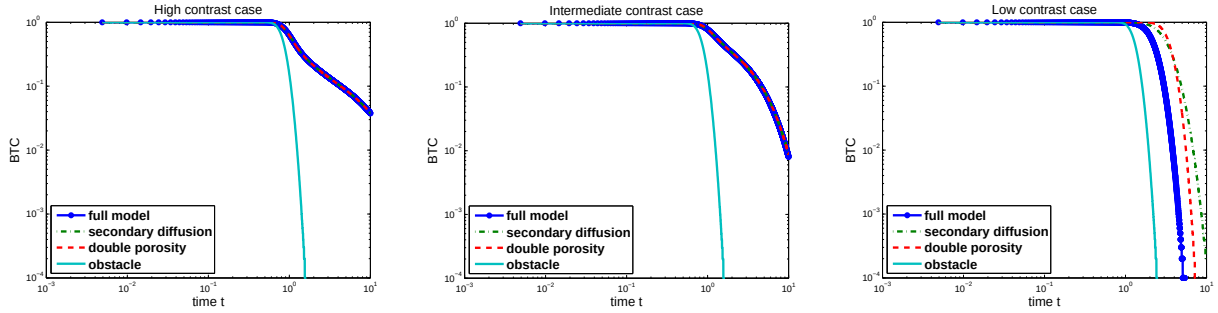

Figure 3: Breakthrough curves using various models on a log-log scale in high, intermediate, and low contrast cases from left to right.

[3] J. Douglas, Jr., and C.-S. Huang, The convergence of a locally conservative Eulerian-Lagrangian finite difference method for a semilinear parabolic equation, *BIT*, **41**, 980–989 (2001).

[4] J. Douglas, Jr., Anna M. Spagnuolo, and Son-Young Yi, The Convergence of a Multidimensional, Locally Conservative, Eulerian-Lagrangian Finite Element Method for a Semilinear Parabolic Equation, *Mathematical Models and Methods in Applied Sciences*, DOI No: 10.1142/S0218202510004246 (2010).

[5] Małgorzata Peszyńska, Analysis of an integro-differential equation arising from modelling of flows with fading memory through fissured media, *J. Partial Diff. Eqs.*, **8**, 159–173 (1995).

[6] Brendan Zinn, Lucy C. Meigs, Charles F. Harvey, Roy Haggerty, Williams J. Peplinski, and Claudius Freiherr von Schwerin, Experimental visualization of solute transport and mass transfer processes in two-dimensional conductivity fields with connected regions of high conductivity, *Environ Sci. Technol.*, **38**, 3916–3926 (2004).